Romanian Reports in Physics **69**, 703 (2017)

STUDY OF FOG EVENTS USING REMOTE SENSING DATA

F. TOANCA[1,2], S. STEFAN[1], L. LABZOVSKII[1,2], L. BELEGANTE[2], S. ANDREI[2], D. NICOLAE[2]

[1]University of Bucharest, Faculty of Physics, PO BOX MG 11, Magurele-Bucharest, Romania
[2]National Institute of Research and Development for Optoelectronics INOE 2000, Magurele-Bucharest, Romania

Received April 21, 2015

Abstract. Fog is a phenomenon that causes a reduction in visibility, a real obstacle for land, air and sea traffic and therefore has a high economical impact. The aim of this paper is to study fog generation conditions using ceilometer data and vertical profiles of temperature and humidity from radiosounding and Microwave Radiometer HATPRO. Mean sea level pressure and geopotential patterns were used as additional information. The study focused on 2012–2014 period characterized by several fog events over for Magurele location (44.35 N, 26.03 E). The results of this study showed that the dominant fog type is radiation fog.

Key words: fog, remote sensing, radiosounding, temperature, humidity, vertical profiles.

1. INTRODUCTION

Fog is a phenomenon that reduces horizontal visibility to less than 1000 m due to the suspended water droplets [1]. Considering this, low visibility meteorological conditions produced by fog have important negative effects on society. For example, total economic loss related to fog is comparable with that for tornadoes, even comparable to that for hurricanes or winter storms in some situations [2]. Fog was studied throughout the years on several field campaigns under different topographic and atmospheric characteristics as Italy [3], Netherlands [4], Canada [5]. Active and passive remote sensing equipments were tested during these campaigns. Remote sensing has the capacity for continuous observation and allows monitoring the temporal evolution of the measured parameters at high temporal resolution. On the other hand, remote sensing measurements depend to some extent on the meteorological conditions. Hence, remote sensing instruments are complementary to radio soundings and provide information of great value between two radio soundings [6]. Active remote sensing equipments like ceilometers use a wavelegth at 0.910 μm with low energy power in order to measure cloud and fog layers [7, 8]. Ground based microwave radiometer (MWRP) may be used to retrieve temperature and relative humidity [9, 10, 11, 12,

13, 14] by using statistical algorithms [15]. MWRPs have been used in many research projects the results showing the advantages of continuous measurements of temperature and humidity [16, 17, 18, 19, 20, 21, 22]. Sanchez *et al.* [23] compared microwave radiometer and radio-sounding data during precipitation and non-precipitation days. The correlation coefficients of temperature are of the order of 0.99 and for humidity take values between 0.90 and 0.96. Remote sensing measurements and models were used in many studies, [24, 25, 26, 27] in order to understand the microphysical and meteorological process in fog formation. Radiosonde – radiometer temperature bias and standard deviation reported over seasonal time periods are less than 2.5^{o} C from the surface to 10 km height [28, 29, 30]. Combining radiometer measurements with data from other instruments such as ceilometers, provide considerable scientific results [31, 32]. A fog study made by Nowak *et al*. (2008) [26] regarding ground based remote sensing equipments showed excellent efficiency for ceilometers as in 98% of the fog situations and 89% of the low stratus situations. The combination of data from active, passive and *in situ* sensors is the most promising way to achieve success in profiling thermodynamic variables throughout the full depth of the troposphere [33, 34]. Fog formation and dissipation are hard to forecast considering the fact that are determined by local meteorological conditions near surface but also by synoptic condition [35]. In Romania, there are few studies about fog but none of these papers are related to ground remote sensing instruments [36, 37, 38, 39].

The main objective of this study was to analyze temperature and humidity vertical profiles obtained from the microwave radiometer for 57 fog events in connection with ceilometer and radio sounding measurements, in order to determine fog events characteristics that occur over Magurele area. In addition, meteorological conditions related to synoptic patterns were also used.

The paper is organized as follows: section 2 describes data and methodology used in this study; Section 3 presents the results related to comparison of MWRP – Radiosounding temperature and humidity vertical profiles and the analysis regarding fog types over Magurele area. The last section of the paper is dedicated to concluding remarks.

2. DATA AND METHODOLOGY

Data and methods regarding fog occurence emphasized by the images of the backscatter profiles offered by a VÄISALA CL31 Ceilometer together with temperature and humidity profiles provided by a ground based Microwave

Radiometer HATPRO for the atmospheric layer (0–10 km) were used. Remote sensing instruments used in this study are installed in a suburban area located in south-western part of Bucharest (Magurele – 26.029E, 44.348N, ASL: 93 m), at Faculty of Physics and Romanian Atmospheric Observatory – National Institute of R&D for Optoelectronics INOE 2000. The studied area is located at 70 km north of Danube River and has as an eastern neighbour Black Sea at 230 km.

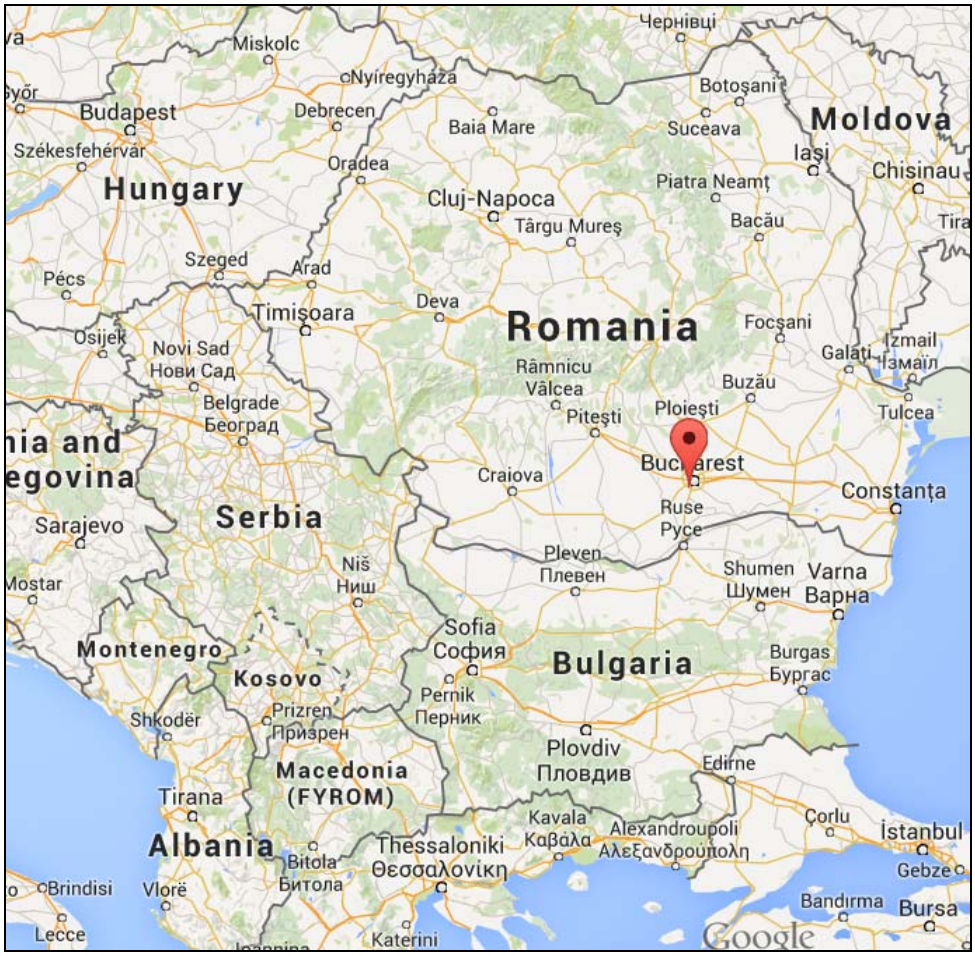

Fig. 1 – Study area map (https://www.google.ro/maps/place/Măgurele).

This region has a temperate – continental climate with four seasons and characterized by the clear differentiation between summer and winter. There are various sources of atmospheric aerosol in the area originating in agriculture, dust,

biomass burning, forest vegetation [40], aerosol representing an important factor for fog occurency.

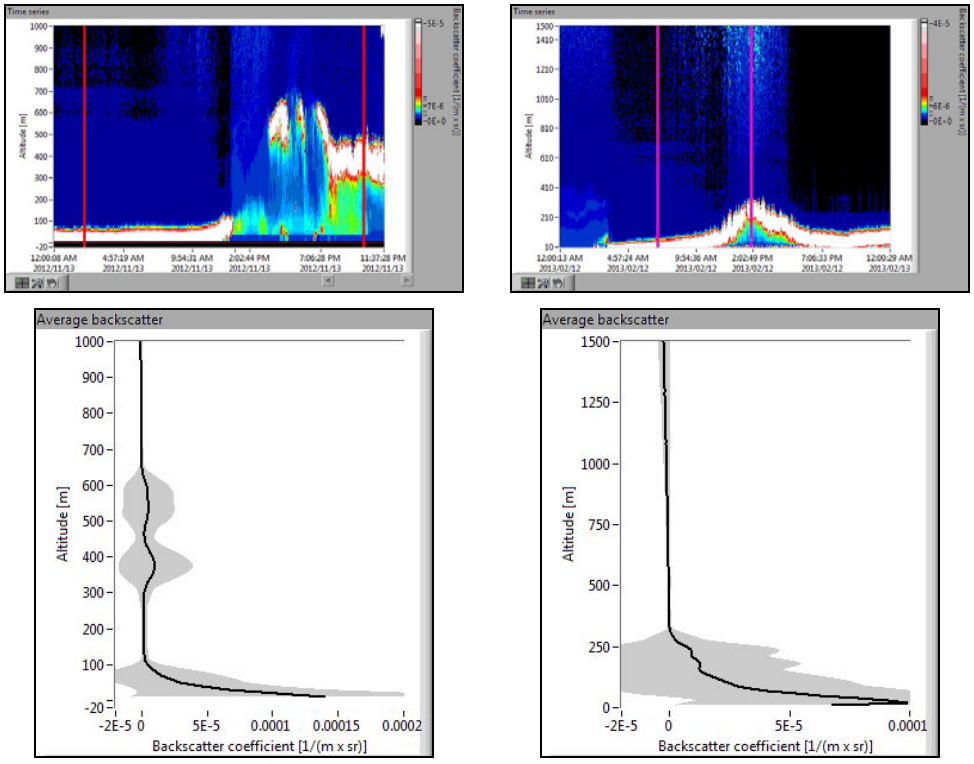

Fig. 2 – Image of fog temporal evolution (upper panel) and associated backscatter profile (lower panel) for November 13, 2012 and February 11, 2013 fog events determined by Ceilometer CL31 VÄISALA.

Fog events occurred during autumn–winter periods of 2012–2013 and 2013–2014 had been monitored with an active remote sensing equipment VÄISALA Ceilometer CL31, which operates much as a lidar. It is installed at Faculty of Physics (Magurele, Romania) and measures continuously in all weather conditions. This device works at 910 nm wavelength, providing backscattering profiles at every 16 s and it goes up to 7.5 km altitude. For ceilometer data visualization and txt format data converting, we used Cloud View software, a graphical user interface created by VÄISALA Company especially for this instrument. There was also created an algorithm using LabView software in order to show fog presence, cloud bases and backscattering profiles.

A detailed description of VÄISALA CL31 Ceilometer is given by [41]. In this study, ceilometer backscatter information is evaluated by comparison with parallel measurements from the microwave radiometer and radio-sounding.

Time evolution of temperature and relative humidity vertical profiles were measured by a passive remote sensing equipment, microwave radiometer (MWRP). The profiling radiometer works at 14 frequencies of the microwave spectrum, in nearly all weather conditions. The MWRP measures the microwave radiance, expressed as brightness temperature, having two bands 22–31 GHz (7 channel filter bank humidity profiler) and 51–58 GHz (7 channel filter bank temperature profiler). For manipulation, averaging and representing the microwave radiometer data, an automatic LabView algorithm has been developed. The algorithm is able to extract the hourly averages of temperature and humidity profiles and to display time series representations of temperature and humidity profiles up to 10 km, over 24 hour time intervals. Due to the complexity of the retrieving method and the sensitivity of water measurements to the fine details of microwave absorption features, some uncertainties can arise. A more general description of ground based radiometric profiling of temperature and humidity is provided by Westwater [42], and obtained temperature and relative humidity data from a microwave radiometer are discussed by Hogg *et al*. (1983) [43].

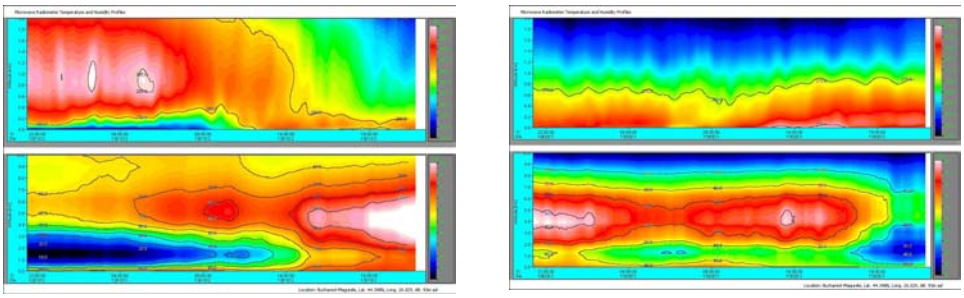

Fig. 3 – Image of fog temporal evolution for temperature T (K) (upper panel) and relative humidity RH (%) (lower panel) for November 13, 2012 and February 12, 2013 fog events determined from MWRP.

RPG HATPRO Microwave Radiometer ASCII files of averaged temperature, relative humidity and absolute humidity profiles are also available. In order to make a comparison between radio sounding and microwave radiometer vertical profiles for 00:00 hour, another LabView algorithm was created for having a common MWRP and radio sounding spatial resolution by interpolating radiosonde profiles to the microwave radiometer height scale. To continue on to the comparison at 00:00 hour we took the retrievals from the MWRP between 23:30UTC to 00:30UTC and we calculated the average values in order to obtain mean temperature and relative humidity profiles at 00:00 UTC. Microwave

Radiometer measurements were performed at the Romanian Atmospheric Observatory (Magurele, Romania).

Radio sounding data from Bucharest station of Romanian's National Meteorological Administration were available from the University of Wyoming [44].

Observational data (human eye observations) related to the state of the atmosphere and meteorological conditions were also performed for whole studied period.

During the period Ocober–March of 2012–2014 a number of 57 fog events (27 events during 2012–2013 and 30 events during 2013–2014) had been detected.

The methodology used in this study follows three steps:

– The comparison of vertical profiles of temperature and humidity from two different sources (MWRP and radio sounding) for a significant number of fog events with the aim to establish whether MWRP profiles could be a reliable, alternative and less expensive data source than atmospheric sounding. The study was made only at 00 UTC;

– The analysis of vertical profiles from Ceilometer CL31 and MWRP together with synoptic patterns to determine fog characteristics;

– The extraction of criteria in charge with fog type generation for Magurele area.

3. RESULTS AND DISCUSSIONS

The study of fog occurrence at Magurele site (44.35 N, 26.03 E) was possible due to the collocation of active and passive remote sensors. Because there was no possibility to perform radio sounding measurements at Magurele, the calibration of MWRP had been done using Romanian National Meteorological Administration radio sounding data. In this study, VÄISÄLÄ CL31 ceilometer was used to emphasize fog evolution, while the temperature and humidity profiles were picked up from the HATPRO microwave radiometer. MWRP was calibrated against radio soundings. Fog characteristics were determined especially related to vertical profiles of temperature and humidity and to synoptic patterns.

3.1. TEMPERATURE AND HUMIDITY VERTICAL PROFILES COMPARISON BETWEEN MWRP AND RADIO SOUNDING

A comparison of 00 UTC profiles (focusing on the lower 1 km) for 57 cases was done in order to determine MWRP data reliability to replace vertical profiles obtained by radio soundings. Temperature and specific humidity values are plotted as a function of altitude. Overall, radiometer *versus* radio sounding profiles revealed a good agreement for the analyzed fog events. Figure 4 shows the

comparison between MWRP and radio soundings temperature and specific humidity profiles for a selection of days with fog. A first result is related with altitude; it can be observed that in Planetary Boundary Layer, the differences are larger than in the free atmosphere as was expected. But is remarcable that in the first 100 m, MWRPs vertical profiles of temperature are similar with those of radio sounding and detected all lower thermal inversions. Temperature inversions for these cases are the results of prolonged radiative cooling and subsidence associated with a persistent anticyclone. In case of specific humidity vertical profiles there are differences in values, but this conservative parameter has same vertical trend evolution for both instruments (Fig. 4, lower panel).

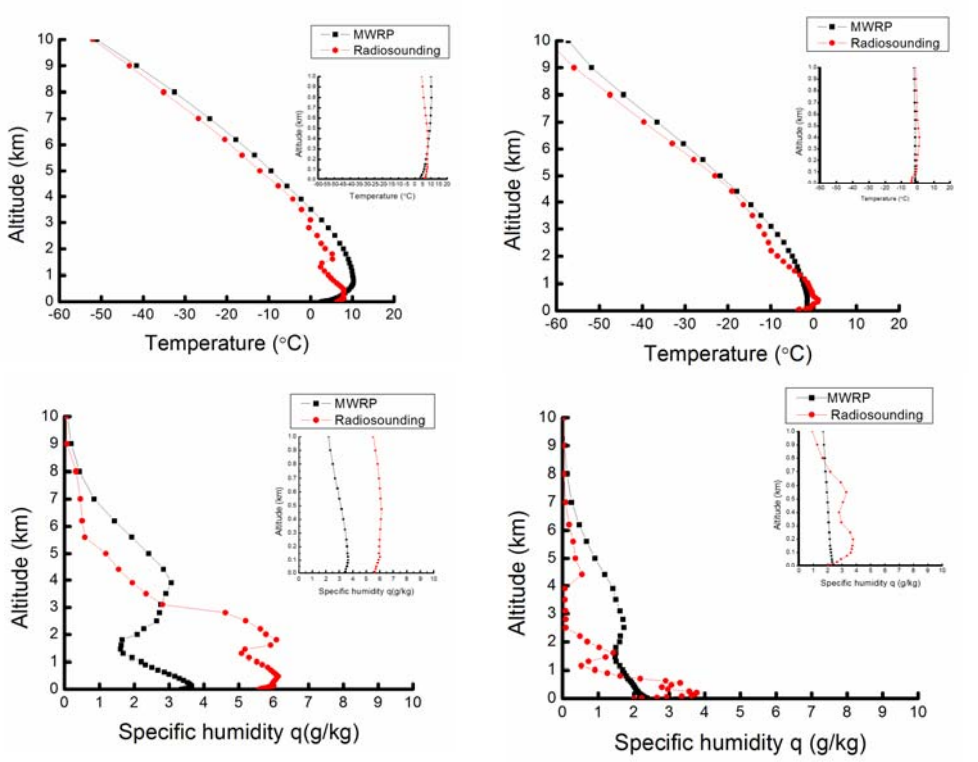

Fig. 4 – Vertical profiles of temperature T (˚C) (upper panel) and specific humidity q (g/kg) (lower panel) from MWRP and radio-sounding for November 13, 2012 (left) and February 12, 2013 (right) for 00UTC.

Even MWRP – radiosonde study showed a good agreement, there are still systematic temperature and humidity differences between microwave radiometer and radio sounding profiles. The differences could be explained by instrumental offsets, absorption model used in the MWRP retrieval algorithms and also by using non representative data sets [45].

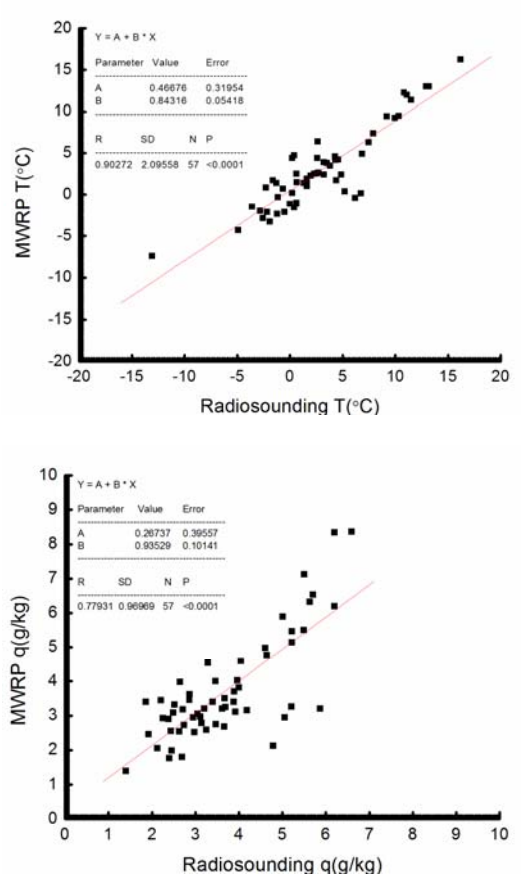

Fig. 5 – Radiosounding *vs* Radiometer temperature (˚C) (left panel) and specific humidity (g/kg) (right panel) correlation for 2012–2013 and 2013–2014 autumn winter period for 00UTC.

Temperature and specific humidity comparisons for first 1000 m have been made between radiosonde and microwave radiometer data for the 57 fog events that occured during 2012–2014 autumn–winter periods. Figure 5 shows a scatter plot comparing data recorded by the MWRP and radiosounding. The correlation coefficient is 0.90 for 2012–2014 autumn–winter foggy days temperature profiles and 0.77 for specific humidity profiles.

3.2. ANALYSIS OF THE FOG EVENTS

The vertical profiles of temperature and humidity from MWRP and backscatter vertical profiles from ceilometer CL 31 together with synoptic patterns

were analyzed to determine the dominant fog type over Magurele for 2012–2014 autumn–winter periods.

3.2.1. Identification and temporal variability of fog events

Observational data represented our start point for data selection. The temporal evolution of air temperature and humidity together with ceilometer backscatter coefficient profiles were examined in order to decide about identification of fog generation and for the criteria to distinguish radiation fog events. Ceilometer's images and backscattering time series confirmed 100% of all fog events noticed by observational data (human eye observations).

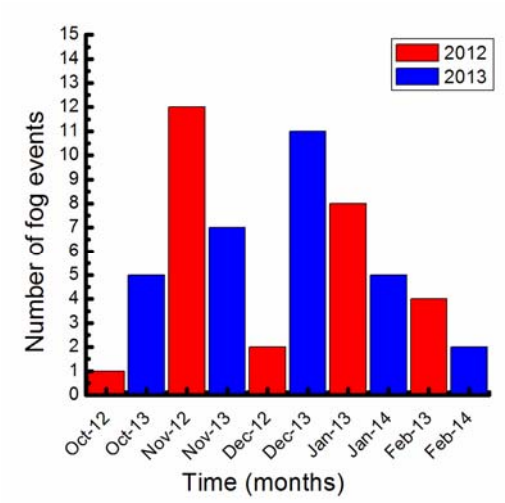

Fig. 6 – Fog events frequency for 2012–2013 and 2013–2014 from VÄISALA Ceilometer CL31.

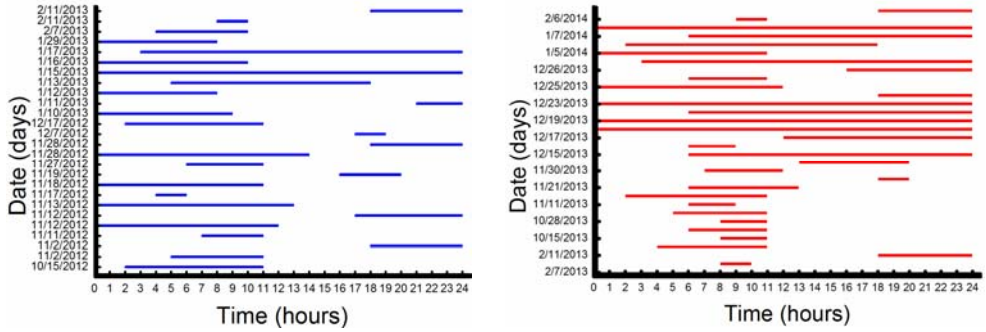

Fig. 7 – Duration of events (number of hours) for 2012–2013 (left) and 2013–2014 (right) autumn–winter periods determined from VÄISALA Ceilometer CL31.

Fog events are first investigated by examining the number of days (Fig. 6) per year and also the number of hours (Fig. 7) per event. It was noted that the fog top was between 50 and 70 m.

Table 1

Fog duration/Number of fog events

Fog Duration (hours)	**02–05**	**06–10**	**11–15**	**16–24**
Number of cases (%)	29.83	33.33	15.79	21.05

The duration of a fog event is considered one of the most important feature of this phenomenon. Therefore it has been evaluated for all the considered events. The results emphasized that the average duration of fog event is 11 h. The duration for different time intervals was as follows: 2–5 hours for 29.83% of cases, 6–10 hours for 33.33% of cases, 11–15 h for 15.79% of cases and 16–24 h for 21.05% of cases (Table 1). The most long lived fog events occured in January 2013, December 2013 and January 2014. Fog is considered a common event for both autumn–winter analyzed periods. On a monthly basis, for the season 2012–2013, November 2012 is the most prone month (12 fog events) while for 2013–2014 in December 2013 had the highest number of fog events (11 fog events).

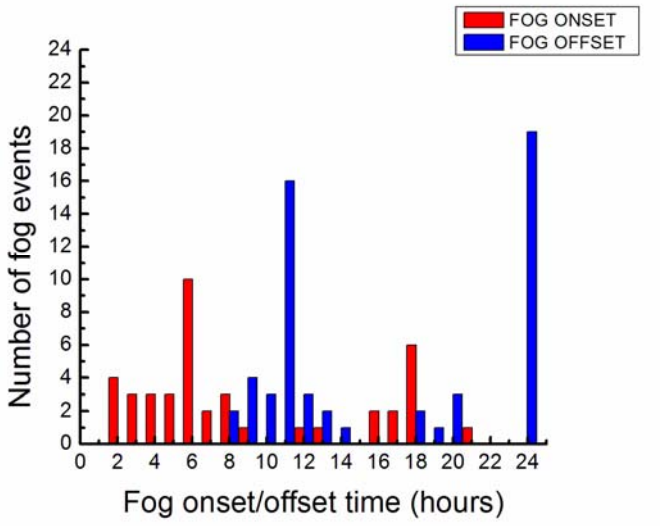

Fig. 8 – Frequency of fog events onset and offset for both seasons (2012–2013 and 2013–2014).

Temporal distribution of fog events in Magurele area is limited to the period between October to February. The distribution of events duration are shown in Fig. 8.

Table 2

Fog onset time/Number of fog events

Fog onset time (hours in UTC)	**00–03**	**04–07**	**08–11**	**12–15**	**16–19**	**20–24**
Number of cases (%)	38.60	31.60	7.00	3.50	17.55	1.75

On a diurnal basis, the highest frequency of fog onset is observed after midnight between 00 to 03 UTC with a frequency of 38.60% and also in the early morning between 04 and 07 UTC with a frequency of 31.58%. So more than 50% of fog onsets occurrs during nightime (Table 2). The explanation is related to the decreasing of air temperature during night and especially in the morning hours. The temperature decreasing initiates the condensation process of water vapor on cloud condensation nuclei (CCN).

Table 3

Fog offset time/Number of fog events

Fog offset time (hours in UTC)	**06–09**	**10–13**	**14–17**	**18–21**	**22–24**
Number of cases (%)	12.28	42.11	1.75	10.53	33.33

The event of fog dissipation is due to enhanced of air circulation, the timing being distributed between 10 to 13 UTC for 42.11% of cases. This means that insolation destroy the morning thermal inversion.

3.2.2. MWRP and synoptic data analysis

MWRP temperature and humidity analysis of 57 fog events were evaluated. Other meteorological variables: radio sounding temperature (T), dew point temperature (Td) and wind speed were also analyzed.

Table 4

Values for selected surface meteorological parameters characterizing the fog events analyzed

Case number	T–Td (°C)	RH (%)	Wind Speed (m/s)	Synoptic patterns
40	0.5–2.1	76.4	≤ 3	HIGH
17	0.5–2.4	74.8	≤ 4.7	LOW

Information regarding mean sea level pressure (MSLP) have been added in order to establish the pressure regime during the fog events. If the atmospheric pressure registered in the vicinity of measurements site was above 1015 hPa, then a high pressure regime was considered (HIGH), and when MSLP was below to 1015 hPa, the pressure regime has been considered to be low (LOW) (Table 4). The high pressure system dominated the analyzed fog events with 70.17% of the total episodes and 29.83% low pressure cases.

4. CONCLUSIONS REGARDING FOG EVENTS CHARACTERISTICS OVER MAGURELE AREA

The complex analysis performed using remote sensing equipments and observational data allowed gathering the most important characteristics for fog generation and dissipation over Magurele. These can be summarized as follows:

Fog occurs during autumn–winter periods, the earliest month being October and the latest is March.

The highest frequency of fog onset is observed in the early morning between 04 and 07 UTC.

The highest frequency of fog offset is distributed generally between 10 to 13 UTC due to influence of solar radiation that destroy the thermal inversion.

The longest fog event had a lifetime of 11 hours but the average is between 6 to 10 hours.

The high pressure system (over 1015 hPa) associated with an anticyclone or anticyclonic ridge dominated the analyzed fog events with 70.17% (Table 4) of the total episodes and 29.83% (Table 4) low pressure cases.

T–Td values are ranging between 0.2 ^{o}C and 4.6 ^{o}C.

RH values ranging between 68.8% and 84.6% emphasized that condensation processes are responsible for fog generation as was expected due to atmospheric aerosol presence over Plain of Magurele.

Considering all these characteristics, the most important conclusion is that the dominant type of fog that occur over Magurele is radiation fog. Fog events occurrence during undefined pressure systems is due to air masses transport. All these results are considered clear criteria that allow us, knowing the meteorological parameters, to estimate fog generation and dissipation.

Acknowledgments. The research of the author L. Labzovskii leading to these results has supported from the European Community's FP7 – PEOPLE 2011 under grant agreement number 289923 – ITARS (Initial Training for Atmospheric Remote Sensing). The work of the author F. Toanca was supported by the strategic grant POSDRU/159/1.5/S/137750, "Project Doctoral and Postdoctoral programs support for increased competitiveness in Exact Sciences research" co-financed by the European Social Found within the Sectorial Operational Program Human Resources Development 2007–2013.

REFERENCES

1. World Meteorological Organization, *International Meteorological Vocabulary*, WMO, Geneva, Switzerland, 1996.
2. I. Gultepe, R. Tardif, S.C. Michaelides, J. Cermak, A. Bott, J. Bendix, M.D. Muller, M. Pagowski, B. Hansen, G. Ellrod, W. Jacobs, G. Toth and S.G. Cober, Pure Appl. Geophys. **164**, *6–7*, 1121–1159 (2007).
3. S. Fuzzi, M.C. Facchini, G. Orsi, J.A. Lind, W. Wobrock, M. Kessel, R. Maser, W. Jaeschke, K.H. Enderle, B.G. Arends, A. Berner, I. Solly, C. Kruisz, G. Reischl, S. Pahl, U. Kaminski, P. Winkler, J.A. Ogren, K.J. Noone, A. Hallberg, H. Fierlinger-Oberlinninger, H. Puxbaum, A. Marzorati, H.-C. Hansson, A. Wiedensohler, I.B. Svenningsson, B.G. Martinsson, D. Schell, H.W. Georgii, Tellus B **44**, 448–468 (1992).
4. P.G. Duynkerke, P.J. Jonker, A. Chlond, M.C. Van Zanten, J. Cuxart, P. Clark, E. Sanchez, G. Martin, G. Lenderink, J. Teixeira, Bound.-Layer Meteor. **92**, 453–487 (1999).
5. I. Gultepe, G. Pearson, J.A. Milbrandt, B. Hansen, S. Platnick, P. Taylor, M. Gordon, P. Oakley, and S.G. Cober, Bull. Amer. Meteor. Soc. **90**, *3*, 341–359 (2009).
6. A. Haefele, E. Maillard Barras, O. Maier, D. Ruffieux, and B. Calpini, ISTP Proceedings, 2012.
7. M. Haeffelin, T. Bergot, T. Elias, R. Tardif, D. Carrer, P. Chazette, M. Colomb, P. Drobinski, E. Dupont, J-C. Dupont, L. Gomes, L. Musson-Genon, C. Pietras, A. Plana-Fattori, A. Protat, J. Rangognio, J-C. Raut, S. Rémy, D. Richard, J. Sciare, and X. Zhang, Bull. Amer. Meteor. Soc. **91**, 767–783 (2010).
8. I. Gultepe, B. Zhou, J. Milbrandt, A. Bott, Y. Li, A.J. Heymsfield, B. Ferrier, R. Ware, M. Pavolonisi, T. Kuhn, J. Gurka, P. Liu, and J. Cermak, Atmos. Research **151**, 2–19 (2015).
9. R. Ware, D. Cimini, E. Campos, G. Giuliani, S. Albers, M. Nelson, S.E. Koch, P. Joe, S. Cober, Atmos. Res. **132-133**, 278–290 (2013).
10. M.P. Cadeddu, J.C. Liljegren, and D.D. Turner, Atmos. Meas. Tech. **6**, 2359–2372 (2013).
11. D. Cimini, E. Campos, R. Ware, S. Albers, G. Giuliani, J. Oreamuno, P. Joe, S.E. Koch, S. Cober, and E. Westwater, IEEE Trans. Geosci. Remote Sens. **49**, *12*, 4959–4969 (2011).
12. L. Bianco, D. Cimini, F.S. Marzano, and R.Ware, Atmos. Ocean. Technol. **22**, 949–965 (2005).
13. F. Solheim, J. Godwin, E. Westwater, Y. Han, S. Keihm, K. Marsh, and R. Ware, Radio Science **33**, 393–404 (1998).
14. K.R. Knupp, R. Ware, D. Cimini, F. Vandenberghe, J. Vivekanandan, E. Westwater, T. Coleman, D. Phillips, J. Atmos. Ocean. Technol. **26**, *6*, 1057–1073 (2009).
15. R.M. Hoff, R.M. Hardesty, F. Carr, T. Weckwerth, S. Koch, A. Benedetti, S. Crewell, D. Cimini, D. Turner, W. Feltz, B. Demoz, V. Wulfmeyer, D. Sisterson, T. Ackerman, F. Fabry, and

K. Knupp, *Thermodynamic Profiling Technologies Workshop Report to the National Science Foundation and the National Weather Service*, NCAR Technical Note NCAR/TN-488+STR, 2012.
16. D. Cimini, T. J. Hewison, L. Martin, Meteorologische Zeitschrift **15**, *1*, 19–25 (2006).
17. D. Cimini, T.J. Hewison, L. Martin, J. Güldner, C. Gaffard, F. Marzano, Meteorologische Zeitschrift **15**, *5*, 45–56 (2006).
18. K. Friedrich, J.K. Lundquist, M. Aitken, E. Kalina, R.F. Marshall, Geophys. Res. Lett. **39**, L03801 (2012).
19. U. Löhnert, O. Maier, Atmos. Meas. Tech. **5**, 1121–1134 (2012).
20. V. Mattioli, E.R. Westwater, D. Cimini, J.C. Liljegren, B.M. Lesht, S.I. Gutman, F.J. Schmidlin, J. Atmos. Ocean. Technol. **24**, 3, 415–431 (2007).
21. D. Spänkuch, W. Döhler, J. Güldner, E. Schulz, Appl. Opt. **37**, 3133–3142 (1998).
22. W.Turner, S. Spector, N.Gardiner, M. Fladeland, E. Sterling, and M. Steiniger, Trends in Ecology and Evolution **18**, 306–214 (2003).
23. J.L. Sanchez, R. Posada, E. Garcia-Ortega, L. Lopez and J.L. Marcos, Atmosph. Research **122**, 43–54 (2013).
24. H. Kokkola, S. Romakkaniemi, and A. Laaksonen, Atmos. Chem. Phys. **3**, 581–589 (2003).
25. D. Baumer, B. Vogel, S. Versick, R. Rinke, O. Mohler, and M. Schinaiter, Atmospheric Environment **42**, 989-998 (2008).
26. D. Nowak, D. Ruffieux, J. Agnew, and L. Vuilleumier, J. of Atmos. and Ocean. Tech **25**, 1357–1368 (2008).
27. S.N. Stolaki, S. A. Kazadzi, D. V. Foris, and T. Karacostas, S., Nat. Haz. and Earth Sys. Sci. **9**, 1541–1549 (2009).
28. J. Güldner and D. Spänkuch, J. of Atmosph. Oceanic Tech. **18**, 925–933 (2001).
29. T.J. Hewison, IEEE Trans. Geosci. Remote Sens. **45**, *7*, 2163–2168 (2007).
30. J.C. Liljegren, S. A. Boukabara, K. Cady-Pereira, and S. A. Clough, IEEE Trans. Geosci. Rem. Sens. **43**, 5, 1102–1108 (2005).
31. P. Herzegh, S. Landolt, and T. Schneider, Proc. 31st Conf. On Radar Meteor., Seattle, Wa, Amer. Met. Soc (2003).
32. R. Rasmussen and K. Ikeda, Proc. 31st Conf. On Radar Meteor., Seattle, Wa, Amer. Met. Soc (2003).
33. B.B. Stankov, Bull. Amer. Meteor. Soc. **79**, 1835–1854 (1998).
34. E.R. Westwater, Bull. Amer. Meteor. Soc. **78**, 1991–2006 (1997).
35. P.J. Croft, R. L. Pfost, J. M. Medlin, and G. A. Johnson, Weather Forecasting **12**, 545–556 (1997).
36. S. Ştefan, D. Borşan, Studii şi cercetări de fizică **42**, *8-10*, 747–754 (1990).
37. S. Ştefan, A. Sima, Rom. J. Phys. **38**, *6*, 607–617 (1993).
38. S. Ştefan, Meteorology and Hydrology **19**, *2*, 23–29 (1989).
39. S. Ştefan, Meteorology and Hydrology **21**, *2*, 17–23 (1992).
40. L. Mihai and S. Stefan, J. Atmos. Oceanic. Techn. **28**, 1307–1316 (2011).
41. C. Münkel, Meteorologische Zeitschrift. **16**, 451–459 (2007).
42. E.R. Westwater, Bull. Amer. Meteor. Soc. **78**, 1991–2006 (1997).
43. D.C. Hogg, M.T. Decker, F.O. Guiraud, K.B. Earnshaw, D.A. Merritt, K.P. Moran, W.B. Sweezy, R.G. Strauch, E.R. Westwater, and C.G. Little, J. Climate Appl. Meteor. **22**, 807–831 (1983).
44. * * *, http://weather.uwyo.edu/upperair/sounding.html.
45. J. Guldner, Atmos. Meas. Tech. **6**, 2879–2891 (2013).